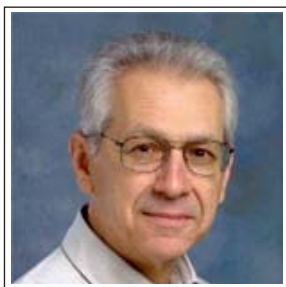


ВЫСОКОПРОЧНЫЕ СТАЛИ ДЛЯ ЭНЕРГЕТИКИ



Лейс Брайан Н., *д.т.н., консультант*
(Уорthingтон, Огайо, США)

Брайан Лейс является известным специалистом в области особенностей распространения трещин в трубопроводах и способах оценки материала противостоять такому разрушению. Публикуемый обзор посвящен решению вышеупомянутой проблемы. В работе представлен научно обоснованный и структурированный опыт решения проблемы распространения трещин в трубопроводах, теоретические изыскания подкреплены анализом нового экспериментального материала, полученного в мире за последние годы в различных странах, включая Россию.

УДК 669.018.298.3

ARRESTING PROPAGATING SHEAR IN PIPELINES

Brian N. Leis, Ph.D., Consultant, Inc. (bleis@columbus.rr.com)

(517 Poe Ave, Worthington, Ohio, 43085-3036, USA)

Abstract. The consequences of what has been termed running ductile fracture require that pipelines be designed to arrest propagation, and so avoid major incidents due to this type of failure. Approaches to characterize pipeline response and their resistance to such failure to ensure arrest rely on semi-empirical models developed in the mid-1970s. Continuing reliance on such semi-empirical models, which were calibrated using full-scale tests done on segments of pipelines, persists because this failure process involves three interacting nonlinearities, and so is complex. These nonlinearities include: 1) plastic flow and tearing instability, 2) soil-structure interaction, and 3) expansion wave response and decompression in the pressurizing media. This paper first reviews the history and related developments that represent almost 40 years invested in fracture-based approaches to quantify propagating shear in pipelines. Graphical evidence of the full-scale failure process and related phenomenology lead to an alternative hypothesis to quantify this failure process that is based on plastic collapse rather than fracture. It is shown that the phenomenology does not support a fracture-controlled process, and that instead the metrics of arrest should reflect the flow properties of the steel. Finally, aspects of fracture-based approaches are related to the collapse-based concept as the basis to understand the success that at times has been achieved using fracture-based approaches. Surrogates for CVN energy that has been used in the BTCM as a measure of fracture resistance are reevaluated as functions of the flow response, which provides the basis to rationalize the historic successes on the fracture-based formulation. Finally, remaining gaps and issues are addressed.

Keywords: propagating shear, fracture, arrest, arrestor, tough steel, Battelle two-curve model, through-wall collapse, plasticity, CVN, DWTT, steel, separations/splits, model development.

Introduction to propagating fracture

The phenomenon historically termed running fracture referred to the rapid axial propagation of a fracture along a transmission pipeline pressurized with natural gas or a super-cooled fluid. Ductile propagation occurs by the axial extension of shear failure (propagating shear) that continues until the decompression front formed in the transported product in the wake of the expansion wave caused by the rupture exceeds the speed of the propagating shear. Arrest occurs because the pressure driving this process falls below its critical value. The balance between the decompression speed and the speeds of the propagating shear is dependent on the fluid's properties, the line-pipe's size and its resistance to failure, and the backfill conditions.

Traits of propagating brittle fracture

The consequences of running fracture require that pipelines be designed to avoid related incidents with a high level of certainty. This was a problem for the line pipe steels of the 1960s and before because offered little resistance to running fracture. In some cases, the steels made prior to the late 1950s had a fracture appearance transition temperature (FATT) well above the service temperature, which opened to the potential for brittle long running fracture. Failed pipes showed chevrons on flat through-wall fracture surfaces, and propagation occurred at very high speeds, well above 500 meters/second (m/s). Multiple fracture paths were common in some full-scale tests and in-service failures, because the energy available to drive fracture often far exceeded the resistance of the steel under such conditions. Brittle propagation tracked a sinusoidal shape that was associated with elastic stress waves triggered by fracture ini-

tiation, which propagated at speeds comparable to the fracture and directed its path(s).

Fig. 1 presents views typical of such cracking that have been adapted for present purposes from archival records of some early work done at Battelle. The traits of brittle propagating fracture are typical of dynamic fracture evident in steels studied in regard to Naval and other structures beginning in the 1940s. Initiation gave rise to a crack that could be seen in high-speed films of the process to extend axially with a sharp crack-tip, consistent with linear-elastic fracture mechanics (LEFM) concepts [e.g., see 1], which had been emerging in the work of Irwin and others in the same timeframe [e.g., 2]. Because the initiated fracture continues to propagate axially, the term “propagating fracture” is physically descriptive of the phenomenology as evident in the high-speed films. Brittle propagating fracture ran in the line-pipe steels of the 1950s and before at speeds the order of the acoustic velocity in the pressurizing media.

The fracture features in Fig. 1, *a* show little evidence of through-wall thinning, while the brittle cleavage mechanism that underlay this process required very little energy to create new crack surface. On this basis, crack advance occurred with very little energy being dissipated per unit area of new surface being created. Fig. 1, *b* is typical of the sinusoids observed, with the amplitude and period of the sinusoid being a function of the pipe diameter and thickness, and other factors that controlled the process.

As the significance of fracture mode was understood, steels were developed that were capable of much lower values of the FATT. Accordingly, the concern for brittle fracture was managed by appropriate steel design and specifications. With the expectation that such ductile steels would end concern for running fracture, full-scale experiments were done to confirm that expectation. But, as history demonstrates, where test circumstances at hoop stresses typical of service led to fracture speeds that outran the decompression front,

dynamic propagation remained a concern. The only difference was that the mode of failure had shifted from brittle to partially or fully ductile. Given that as Figure 1a shows little dissipation occurred in regard to plastic flow local to the fracture plane, arresting this failure process was difficult, with very long fractures possible, some of which ran many miles. Arrest in such cases was plausible only if a reduction in the factors that drive this cracking occurred, due to a decreased hoop stress, or if pipe joints were encountered that had a FATT below the test or service temperature, thereby providing more dissipative properties.

Traits of propagating ductile fracture or propagating shear

Fig. 2 shows the traits of ductile fracture propagation developed in some of the early testing, which as for the prior illustrations have been adapted from archival records in regard to related work by the author. Fig. 2 develops in parallel to the elements of Fig. 1, *a*. Fig. 2, *a* illustrates a transitional situation wherein the steel’s response is partially ductile, whereas Fig. 2, *b* shows traits that were typical of fully ductile response.

The transitional response presented in Fig. 2, *a* shows flat fracture typical of brittle behavior at mid-wall, while shear fracture is evident at the inside and outside surfaces of the pipe. There is very little evidence of through-wall thinning that reflects plastic flow very local to the fracture. Such thinning is only evident over a distance less than one wall-thickness from the plane of the failure. Fig. 2, *b* is typical of the fully ductile response evident for conventional steels produced circa the mid to late 1960s. Although this shows shear response across the full wall thickness, the extent of the through wall thinning is just marginally greater than that evident for the transitional behavior. However, the thinning is limited to about 10 % of the wall thickness and this develops over a distance the order of twice the wall-

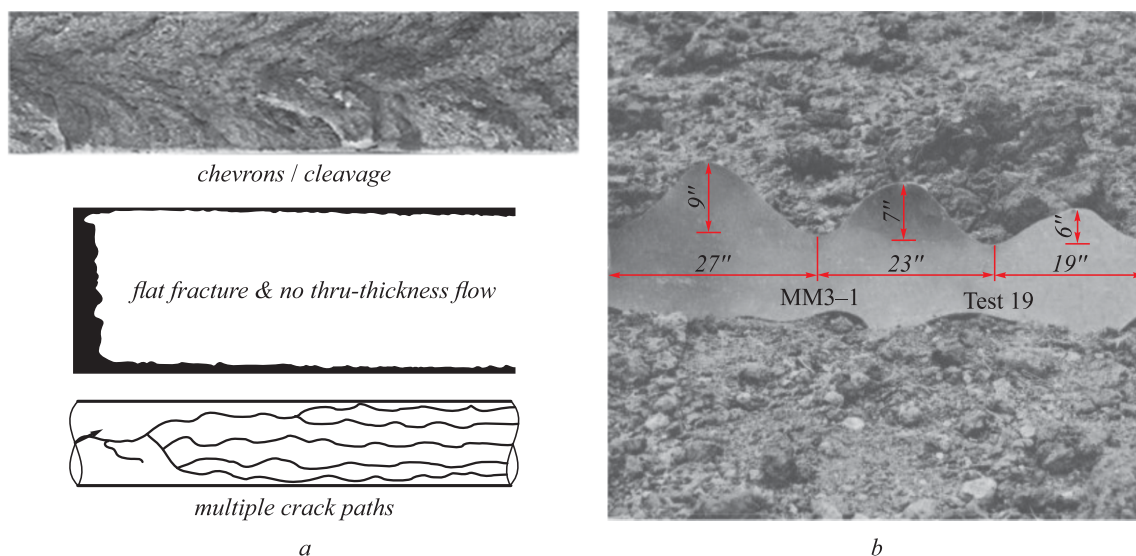


Fig. 1. Traits of brittle propagating fracture – full-scale testing circa 1960:

a – characteristics of the fracture process and path; *b* – post-test photograph of the fracture path indicating the scale the sinusoid in inches

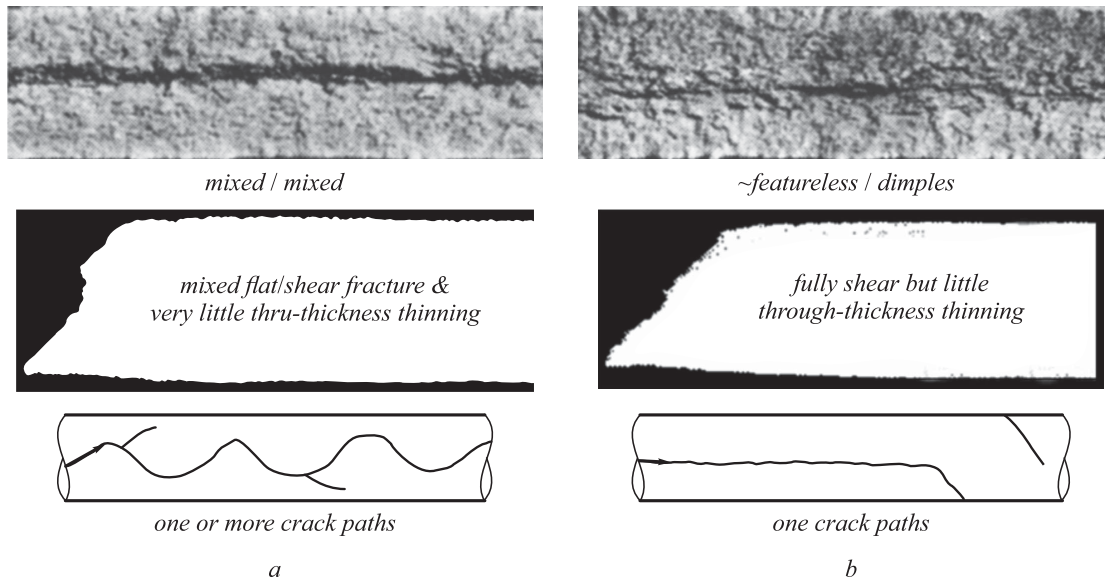


Fig. 2. Characteristics of the fracture process and path for transitional and ductile response: *a* – transitional response circa the mid-1960s testing; *b* – fully ductile response circa the late 1960s testing

thickness from the plane of the failure. As such, even for fully ductile response, the amount of energy dissipation due to plastic flow local to the rupture plane is small, and as the surface is rather featureless the energy required to create new surface is relatively small per unit area created.

Early models characterizing propagating shear failure

Even in the 1960s and early 1970s, a full-scale experiment to quantify the response of the pipeline to possible propagating shear failure was expensive. These experiments also involved significant preparation time and even then success was not guaranteed. Finally, the utility of the outcomes of such tests were limited to the specific steel and experimental parameters evaluated. While these aspects remain the same today as in the 1960s, the passage of time has produced much better instrumentation, with high-rate data capture, and computer-based data management, and analyses. Even so, the high cost when weighed against the limited generality of each full-scale test motivates the development of models that capture the controlling factors to determine if a given steel meets the requirements of a proposed advanced pipeline design.

Rudimentary nonlinear fracture mechanics (NLFM) technology [e.g., see 1] was emerging in the 1960s in parallel with the view that propagating shear failure was a safety concern. Because the available technology then fell well short of addressing the coupled nonlinearities evident in the full-scale testing, it was expedient then to formulate an empirically calibrated semi-analytic model. While NLFM has come a long way since, the complexity of the physics and mechanics means that even today the work on modeling continues to rely on empirical calibration. In this context, while current modeling work appears elegant, in most ways

it is no more fundamental in its formulation than the work done at Battelle beginning in the 1970s.

The battelle two-curve model

Battelle [3] developed independent expressions for the gas-decompression behavior and fracture resistance that were coupled in a model through what was termed a backfill coefficient, denoted herein as C_{BF} . The approach to characterize decompression was analytic and based on the Benedict-Webb-Rubin equation of state (EoS), as modified by Starling [4, 5] (BWRS). This EOS covered a spectrum of gas compositions through inclusion of binary interaction coefficients for natural gas liquids up through C6, and also the presence of CO₂. This fundamentally sound formulation proved viable for the gas compositions of interest then, and remains quite robust today in dealing with the rich (dense-phase) gas compositions of recent interest [e.g., 6]. The speed of the propagating shear failure was expressed analytic functional form based on mechanics analysis for plastic wave propagation. It became empirical through its calibration in reference to both flow properties and fracture resistance for the steels involved. These one-dimensional expressions for the propagating shear speed and the decompression speed and were then empirically coupled through C_{BF} .

Determination of the toughness required for fracture arrest came by identifying the toughness that caused these two independent velocity expressions to become just tangent. As the solution was done graphically, the two curves representing each of the expressions involved, this model became known as the Battelle Two-Curve Model (TCM). This TCM became the standard by which the arrest toughness was determined, and remains in use today by virtue of its being the only simply practical model capable of addressing such situations.

Because the Battelle TCM (BTCM) required an iterative solution, and many of the situations of concern involved single phase or nearly single-phase gases, the BTCM was used parametrically to solve a matrix of cases under the general assumption that the gas was lean and the pipeline was backfilled with soil. The cases considered included: outside diameters from 12 to 48 inches (305 to 1219 mm) and wall thickness, t , ≥ 0.1 inch (2.54 mm); pressures from 594 to 2200 psig (4092 to 15158 kPa) causing hoop stresses from 64 to 80 % of the specified minimum yield stress (SMYS) in the range from 50 to 80 ksi (345 to 551 MPa), and values of the acoustic velocity in the gas at its initial pressure and temperature, V_a , in range from 1200 to 1400 feet/second (ft/s) (366 to 427 m/s). The results of this analysis matrix were then trended, and that outcome evaluated at the average value of V_a over the range considered (i.e., 1300 ft/s or ~ 397 m/s). The resulting equation, termed the Battelle simplified equation (SE) [7], was given as:

$$\begin{aligned} C_{v(1/1)} &= 1.08 \cdot 10^{-2} \sigma_h^2 (Rt)^{1/3} \quad (\text{US Units}); \\ C_{v(1/1)} &= 3.57 \cdot 10^{-5} \sigma_h^2 (Rt)^{1/3} \quad (\text{SI Units}), \end{aligned} \quad (1)$$

in which R is the radius of the pipe; t is as above the wall thickness; σ_h denotes the hoop stress; and C_v denotes the Charpy Vee-notch (CVN) energy and $C_{v(1/1)}$ indicates that it is the linearly scaled full-size equivalent (FSE) CVN energy. This is one of many SEs, with many others including those due to the American Iron and Steel Institute (AISI) [8] and the British Steel Corporation (BSC) [9]. These two along with the Battelle SE underlie the criteria historically listed in various Codes and Regulations for use in assessing arrest requirements.

Limitations and key assumptions inherent in the BTCM

The BTCM and the Battelle SE (BSE) embed empirical calibration for Grade 448 (X65) and below. The steels considered had toughness quantified by the FSE CVN energy of 100 J or less, with the average being less than 35 ft-lb (~ 47 J). Similar limitations on calibration data exist for all SEs, which depend on the specifics of the database that underlies their empirical calibration. The BTCM also embeds limitations on scope that reflect the strength and flow (strain hardening) response and toughness, for both fracture initiation and fracture propagation. Fracture initiation enters the BTCM through consideration of the fracture arrest pressure, which carries back to the log-secant-based NG-18 Equations [10]. Fracture propagation for this formulation embeds parameters that quantify both the deformation response and the fracture resistance.

Two empirical calibrations central to the development of the BTCM are illustrated in Fig. 3 and 4. Fig. 3 presents the correlation developed to relate fracture resistance quantified by CVN energy, presented on the x -axis, to the strain-energy release rate in a pipe, denoted then as G_c , shown on the y -axis. To provide consistent units between these parameters, the CVN energy was presented as an energy density per unit area (i.e., $12 \text{ CVN}/A_v$, where A_v is the area of the CVN specimen in inch^2). The energy release rate G_c for the thin-walled pups tested was defined as K_c^2/E , where K_c denotes the crack-tip stress intensity factor driving fracture, which was taken in the strip-yield form developed by Hahn et al [11] viz.:

$$K_c^2 = \frac{8c\bar{\sigma}^2}{\pi} \ln \sec \left[\frac{\pi\sigma_h}{2\bar{\sigma}} \right], \quad (2)$$

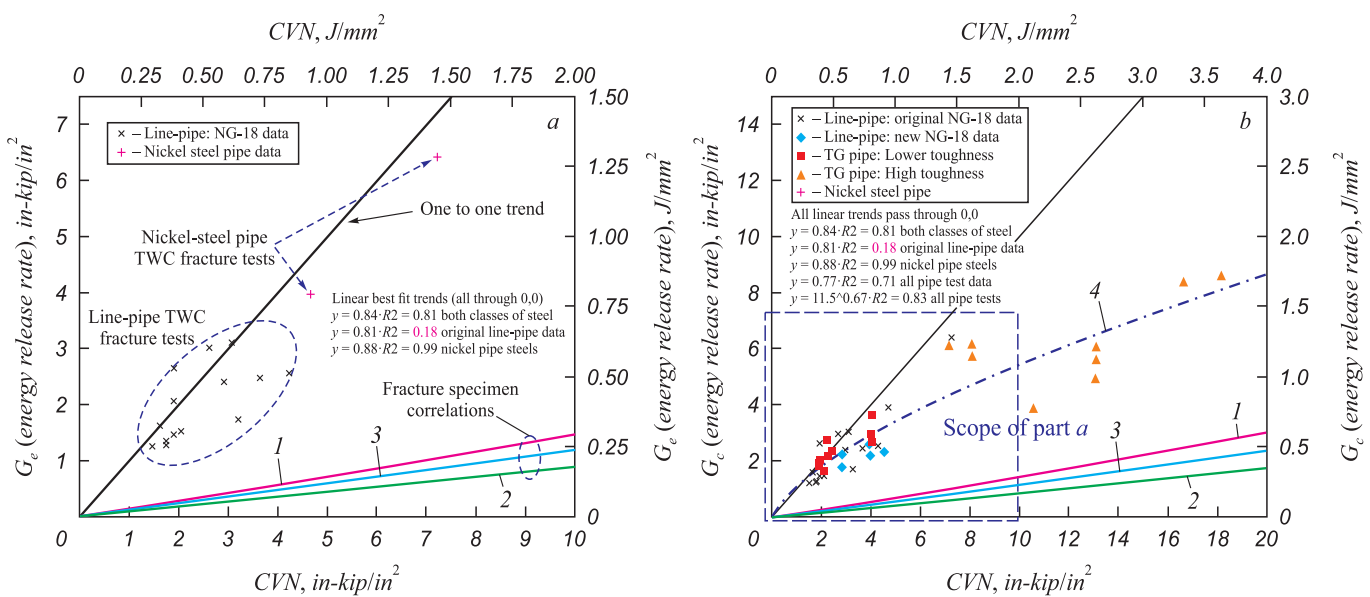


Fig. 3. Correlation between the full-scale test value of G_c and CVN resistance: a – lower toughness results; b – recent higher toughness results; 1 – BS7910 specimen fit; 2 – Barsome&Rolf X52 specimen fit; 3 – Barsome&Rolf X70 specimen fit; 4 – Power-law specimen fit

where $\bar{\sigma}$ was flow stress defined as the actual yield stress, σ_y , plus 10 ksi (69 MPa), σ_h was as above the hoop stress, and c denoted the half-crack length. In turn, these parameters were used to quantify the fracture initiation and propagation resistance, denoted then as R .

Fig. 4 presents the correlation developed to address the effects of backfill and the correlation that was developed to relate the propagating shear velocity to:

- 1) the flow properties of the steel quantified by $\bar{\sigma}$,
- 2) the steel's resistance to fracture, R ,
- 3) the dynamic (instantaneous) pressure on the decompression front, P_d , the arrest pressure, P_a ,
- 4) the backfill coefficient, which was taken to be constant, C_{BF} , and
- 5) a fitting parameter, the exponent denoted "x", viz.:

$$V_F = C_{BF} \frac{\bar{\sigma}}{\sqrt{R}} \left[\frac{P_d}{P_a} - 1 \right]^x \quad (3)$$

In this equation, V_F is the 'fracture' speed, while V_{pl} was the speed of the plastic wave in the pipe steel running in advance of the fracture, and the value of exponent was empirically chosen, as was the constant, C_{BF} . Fig. 4 presents this correlation in terms of normalized pressure on the y-axis, expressed as P_d/P_a , as a function normalized fracture velocity on the x-axis expressed as $V_F/(\bar{\sigma}/(C_v/A_v))^{0.5}$.

Consider first Fig. 3. Fig. 3, a presents the results from Reference 10 that underlie the correlation used in the BTCM between CVN energy density and the corresponding value of G_c quantified by the response of full-scale burst tests on short pups. The values of G_c shown were calculated using the pretest length of the through-wall (TW) defect that was cut into each pipe, which was then sealed against

leaking. Two groups of data points and one set of trends are shown. The small sample of tests involving TW defects (TWD) that were chosen for this calibration are shown as the "X" symbols, while data for two tests of higher-strength (~X80) nickel-steels (specifically IN787) are shown as the "+" symbols. The CVN plateau toughness (CVP) for these steels ran from 15 to 75 ft-lb (20 to 102 J) in grades from X52 through EX100 (358 to 690 MPa), where the EX100 is a 1960s vintage experimental quenched and tempered (Q&T) pipe that remains in service today, although at a value of SMYS dictated by that for the much lower grade pipe it was run with. Although the data showed high scatter that went unresolved, and the best-fit linear slope for all of the data was ~0.81, while that for the line pipe was only 0.18, these results were represented by a one-to-one relationship in the BTCM, and other related modeling.

The linear trends that lie near the lower margin in Fig. 3, a relate CVP to K_c^2/E in terms of broadly published correlations between CVN energy and results for LFM fracture mechanics laboratory-scale test geometries. The disparity between the pipe data and those fracture-mechanics-based correlations is large, which apparently traces to the finite width of those geometries in contrast to the undefined but very large effective width for the pipe. That the specimen-scale correlations do not approach zero as CVN does means they could not be simply scaled to account for the disparity between full-scale and laboratory-scale results.

While the data in Fig. 3, a were considered adequate to empirically calibrate the BTCM for lower-toughness steels, it is clear from Fig. 3, b that the response at higher-toughness cannot be represented by the linear correlation adopted in the BTCM. Fig. 3, b roughly doubles the scales in part a) of this figure, to permit inclusion of recent work by Tokyo Gas (TG) [12] that extends the database to cover toughness values that approach the levels more typical of modern line pipe. It is clear from Fig. 3, b that use of linear correlation in the BTCM is open to question beyond a FSE CVN energy level of about 75 ft-lb (~100 J). The NG-18 Equations that are embedded in the BTCM are likewise limited in their utility to that same energy level. It is apparent given the scatter in Fig. 1, a that the one-to-one correlation can overestimate the fracture resistance of the pipes that underlie this figure by almost a factor of two. Finally, in regard to Fig. 3, b it is apparent that the one-to-one correlation can overestimate fracture resistance to an extent that increases as toughness increases. This tendency is consistent with the 'Leis correction factor' (LCF) for the BTCM [13], which was based on instrumented CVN testing that showed the relative fraction of the energy dissipated in crack propagation decreased nonlinearly as the toughness increased. As noted elsewhere [14], these trends suggest a simple correction to the BTCM based on the trend in Fig. 3, b has the same effect on predicted energy to arrest fracture as does the LCF.

Five key assumptions were implicit in regard to Fig. 3. First, it was tacitly assumed that fracture mechanics char-

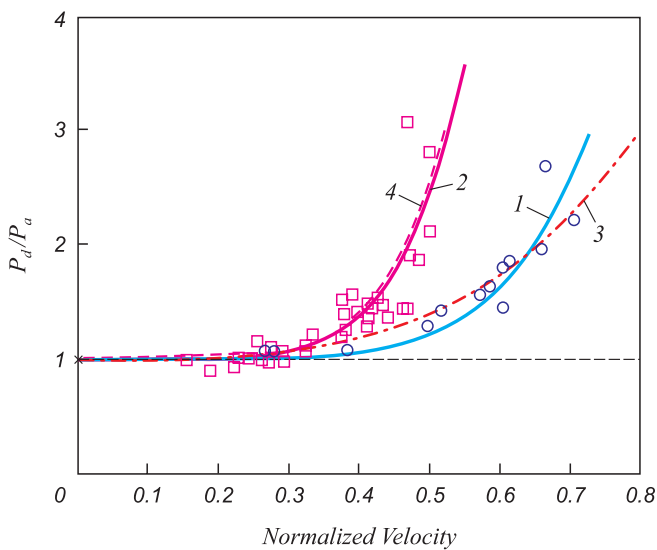


Fig. 4. Relationships between normalized pressure and normalized fracture velocity:
 □ – FS Test, 30-inch backfill; ○ – FS Test, no backfill;
 1 – BTCM, no backfill; 2 – BTCM, 30-inch backfill;
 3 – Lin Reg, no backfill; 4 – Lin Reg, 30-inch backfill

acterized the phenomenology associated with the failure process that Fig. 2 indicates occurs by ductile shear failure, which runs along the pipeline. Second, it was assumed that the strip-yield model for K_c developed by Hahn et al [11] adequately characterized the driving force for this shear failure process. Third, it was assumed that K_c so quantified could be adequately represented in regard to the pretest size of the patched TWDs cut into the pipes reported on in Fig. 3. Fourth, it was assumed that the CVN sample and the energy dissipated quantified adequately characterized the resistance of pipe steel to the propagating ductile shear failure evident in Fig. 2. Fifth, and last, it was assumed that the trend in Fig. 3 could be adequately characterized by a one-to-one relationship between $G_c = K_c^2/E$ and the CVN energy. Discussion in the next section returns to consider several of these assumptions.

Consider next the results presented in Fig. 4, which discriminates between the results from the full-scale testing for soil backfill (“□” symbols) and for no backfill (“○” symbols), and shows the best-fit linear regression for these data as dashed lines. This figure also shows the correlations used in the BTCM to relate fracture velocity to pressure for these datasets and determine the backfill coefficient, denoted CBF. All else being equal, it is apparent that the ‘fracture’ velocity where backfill is present is much less than when the testing is done either in an open trench or above ground – because the data for the backfilled testing lie well to the left in this figure, at lower velocities, than do the results without backfill. Fig. 4 indicates that a high-quality data fit is achieved when the exponent is as chosen at 1/6 across the range of results for nominally 30-inch-deep (762 mm) backfill. This follows from the observation that the regression trend shown as the short dashed line virtually overlays the solid line that derives from the form of Equation 3 when the value of the exponent is taken at 1/6. Simplicity in formulating the BTCM achieved by retaining this value of the exponent for cases where backfill is absent leads to the solid line shown through that dataset. While that choice led to a functional form that passes through or near much of that data, Fig. 4 indicates that this choice falls well off the best-fit line through those points, which is shown in this figure as the dash-dot line.

Several assumptions were also associated with the relationship developed in regard to Fig. 4. First was the fundamental assumption that the fracture process follows in the wake of and can be quantified as a function of the speed of a plastic zone that runs ahead of the propagating shear failure. Second, it was assumed that the three-dimensional (3-D) flow process in the propagating plastic zone could be adequately characterized in a one-dimensional framework by a flow stress and strain hardening exponent (i.e., implicitly typical tensile properties). Third it was assumed that the resistance to propagating shear could be expressed relative to the plastic strain and the flow stress. Fourth it was assumed that Equation 3 adequately characterized this set of parameters. Finally, it was assumed that the two empiri-

cally determined parameters in that context could be taken as constant for a given set of backfill conditions, with the exponent further taken to be the same regardless of the backfill conditions. Discussion in the next section also returns to consider several of these assumptions.

Implications and consequences of the BTCM assumptions

In spite of the many above noted assumptions, and its calibration being limited to steels in Grade 448 (X65) and below that had $C_{v(1/1)}$ energy at 100 J or less, the BTCM remains in use well beyond these limitations. This is because it is the only relatively simple and so practical basis to assess arrest toughness available today. That being said, it is instructive to assess the viability of the many assumptions, to better understand their implications in applications of the BTCM to modern steels. More important practically, because the scatter evident in regard to Fig. 3, *a* and 4 indicates that predictions based on the BTCM will likewise show scatter, it follows that improved predictions would result if the cause of the scatter was understood and could be excised. Quantifying which assumptions drive the scatter thus helps to identify where this effort has the potential to improve arrest predictions within a fracture-based framework.

This section uses the BTCM to predict the required arrest toughness for the line pipe steels and pipe sizes typical of the era when the BTCM was being developed. Two datasets are considered in this assessment of the BTCM. The first involves the dataset that underlies the development and empirical calibration of the BTCM [15]. Given the many disposable parameters involved, and their use in tuning the calibration, the BTCM should correctly calculate the required toughness across that dataset. The second dataset evaluated is that developed in work for the British Gas Council (BGC) [16], which occurred over almost the same period as the testing for the BTCM. Because the work for the BGC involved steels and pipe sizes from the same era, issues due to changes in such parameters over the decades since the BTCM was formulated are eliminated as causes for predictive disparity – if such is found.

Best-case scenario – the BTCM applied to its calibration database

Fig. 5 presents the arrest toughness calculated using the BTCM across the database that underlies its calibration [i.e., 15]. While such calculations are akin to predictions, they are more correctly an assessment of the quality of the curve-fits and the adequacy of the constants chosen for the several disposable parameters. The x -axis in this figure is the FSE CVN energy associated with the pipe that arrested the fracture, while the y -axis is the value calculated by the model. Fig. 5, *a* is specific to the BTCM, while Fig. 5, *b* addresses the results for the BSE applied to the same dataset. Correct results in this format involve arrest results (open circles) that lie below the one-to-one line and

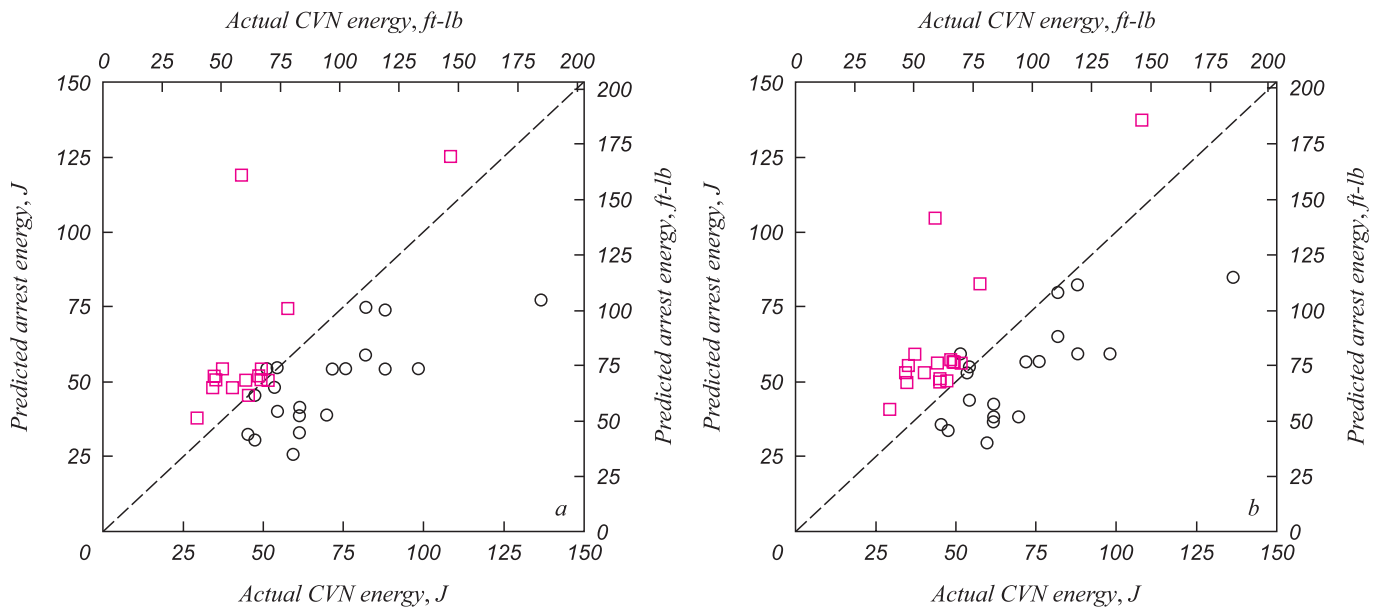


Fig. 5. Calculated arrest toughness for the database that underlies the BTCM calibration: *a* – BTCM calculations; *b* – BSE calculations; □ – propagate; ○ – arrest

propagate results (open squares) that lie above it. While incorrect results that lie on either side of the one-to-one line indicate an issue, those cases where arrest is predicted whereas propagation actually occurs are non-conservative and so pose a significant practical concern, and so hereafter are termed ‘critical errors’. Such critical errors are evident as open circle symbols anywhere above the one-to-one line.

Given the several disposable parameters and the ability to tune the values for the constants in formulating the BTCM, the vast majority of the arrest versus propagate calculations are expected to be correct across its calibration database. Fig. 5, *a*, which presents the results of those calculations confirms this: the results show good discrimination between pipes that arrest or propagate shear failure. Likewise, because the BSE trends predictions based on the BTCM, except for its assumption that the arrest velocity for these tests could be reasonably represented by the average value of 1300 ft/s (397 m/s), good discrimination also is expected for the BSE. Fig. 5, *b* confirms this, but it must be emphasized that all data considered reflect single-phase decompression response.

While the results in Fig. 5, *a* indicate that the disposable parameters and their tuning affected good discrimination across the calibration database, they lead to one critical error where arrest is expected but propagation occurs, while a second case falls just slightly on the error side of the one-to-one line. While this corresponds to a critical error rate the order of a few percent, the several disposable parameters and related tuning suggest that even one critical error is more than might be expected. Because the BSE was derived by trending the BTCM for tests that involved single-phase decompression, the results in Fig. 5, *b* for the BSE are expected to be comparable to that for the BTCM. This is indeed the case, as the critical error rate for the BSE

is identical to that determined for the BTCM. Given the basis for the BSE, this outcome suggests that at least for these full scale tests the value of the arrest velocity for these tests must be close to the value of 1300 ft/s (397 m/s) assumed in regard to the BSE.

It follows from Fig. 5 that the BTCM and the BSE reasonably characterize the propagating shear failure behavior that occurred within their calibration database. Likewise, it is apparent that the many assumptions appear viable – and that the scatter that underlay some of the key assumptions does not significantly impair the model’s ability to discriminate whether a pipe’s properties are capable of arrest versus propagation.

Predictive scenario – BTCM applied to a contemporary database

Consider next the utility of the BTCM and the BSE to predict the arrest toughness required in regard to data developed outside their calibration, but within the same class of steels and pipe sizes typical of the era when the BTCM was developed. To that end the BTCM and the BSE are evaluated relative to predicted values of arrest toughness versus that observed in related full-scale testing done in the work associated with the BGC [16]. Fig. 6 presents these results in the same format adopted for Fig. 5. The only key difference is that the scales on the axis of the figures has been reduced roughly by a factor of two, to accommodate the relatively lower resistance of the steels involved.

The predictions evident in Fig. 6 are comparable to those for the calibration database (Fig. 5) for the cases where the pipe is capable of arresting the propagating shear failure, all of which are correctly predicted, save for one critical error. However, for this dataset that critical error (which is highlighted by the dashed circle) is badly miscalculated – as it

falls far above the one-to-one line in comparison to that in Fig. 5. While similar to the calibration dataset in regard to the arrest results, these true predictions involve many miscalls for pipes where shear failure continued to propagate. These pipes are evident in Fig. 6 as the many square symbols that now fall well below the one-to-one line for both the BTCM and the BSE.

In view of Fig. 6 it is apparent that when the BTCM is used outside its calibration dataset more scatter is evident: six miscalled predictions now are evident out of 24, leading to a rather high error rate of 25 %. Whether or not this outcome is due to scatter, or to differences in the fitting parameters that would better harmonize the combined database, or if the relatively lower toughness steels considered in the BGC work involved fundamentally different response is unclear. While one critical error occurred as for the calibration database, five pipes were predicted to propagate whereas arrest occurred. It follows that the BTCM did not effectively discriminate between an arrest versus a propagate pipe – which is its primary function. In addition, the extent of disparity between the predicted outcome and the actual response increased somewhat. The

next section considers one major error source as a possible explanation for this.

Assessing a major source of scatter

Detailed study of the underlying calibration database suggests that the significant scatter evident in Fig. 3, *a* is due to the assumption (or expectation) that the pretest notch length was a viable estimate of the length at instability. The extent of the error that can be ascribed to this assumption can be inferred in regard to Fig. 7 (adapted from [14]), which is a view local to a patched TWD in a thin-walled pipe made of a 1964 vintage line-pipe steel. Many such tests were done then [e.g., 10] as well as since involving larger-diameter relatively thin-wall pipes, using notches whose pretest lengths ranged from $0.1 \leq c^2/Rt \leq 20$.

The image in Fig. 7 reflects Test #18-8 on a 30-inch (762 mm) diameter pipe, with 0.375 inch (9.53 mm) wall made of grade X52 (358 MPa). This line pipe had an actual yield stress (AYS) of 60.6 ksi (418 MPa) and an ultimate tensile stress (UTS) of 81.3 ksi (560 MPa), leading to $AYS/SMYS = 1.165$ with $Y/T = 0.75$, all of which are typical of the late 1960s TWD database. The pretest length

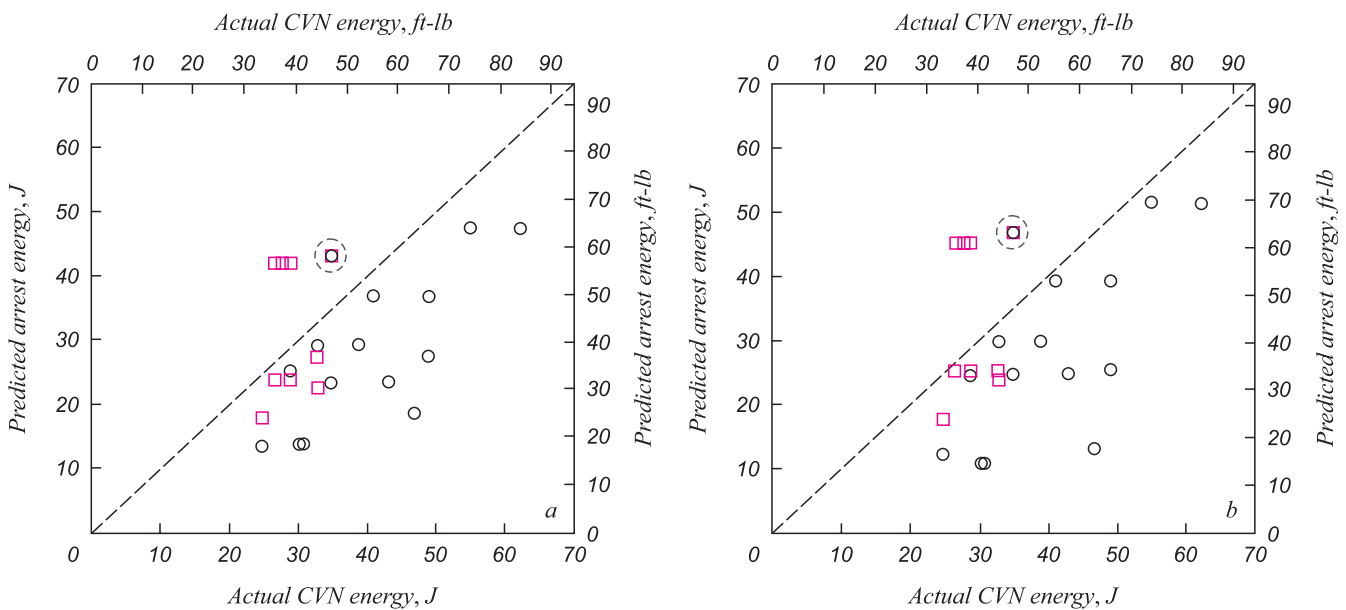


Fig. 6. Predicted arrest toughness for the BGC database: *a* – BTCM predictions; *b* – BSE predictions; □ – propagate; ○ – arrest

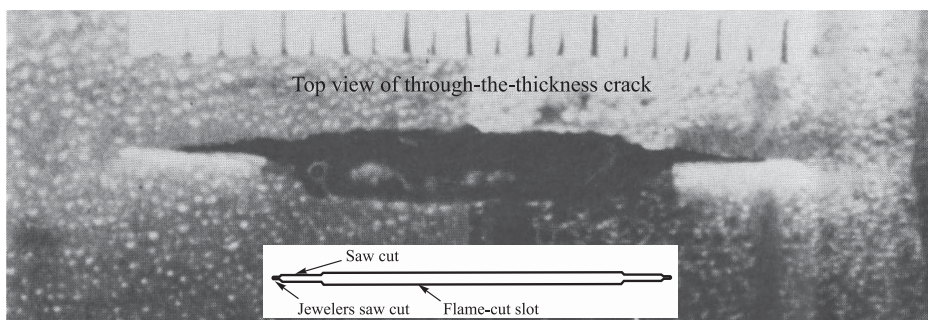


Fig. 7. View of a TWD seconds prior to instability (the inset indicates the pretest notch length)

of this TWD, whose tips were cut with a jeweler’s saw, was 3.3 inches (84 mm) for which c^2/Rt 0.49. As such, this TWD was rather short in comparison to the range of pretest lengths that were evaluated. This defect was patched to seal against leaks and pressurized until axial instability of the TWD, which occurred at $1.07 P_{smys}$. The temperature for this test was 26 °F (3.3 °C), which opens to the potential for less ductile response, as it falls well below the shear-area transition temperature (SATT). That being said, because this pipe had a relatively high CVP energy at that temperature, collapse-controlled failure remained plausible.

Test 18-8 was captured on high-speed film through instability, from which Fig. 7 and a sequence of like images was obtained – with that shown made just seconds before instability. Although the testing was done below the SATT, it is apparent from Fig. 7 that significant subcritical tearing developed prior to instability. Also note that the NG-18 Equations that figure prominently in aspects of the BTCM incorporate bulging local to defects, which appears as an important factor. While that could be the case for some tests involving longer TWDs, it is apparent in Fig. 7 (and many others like it) that the image remained in focus as is apparent here up through instability. Given that bulging involves deformations that locally distorts the pipe’s cylindrical shape, the image quality here implies that the pretest focus remained viable.

It follows that little local bulging occurred, which opens to question when the significant pucker often seen post-test actually forms, and the extent to which bulging prior to axial instability contributes to that posttest pucker. But, more critically in regard to Fig. 3, which discounted possible growth through use of the pretest TWD length in calculating G_c , Fig. 7 shows that significant differences can develop between the calculated and actual values of G_c , which lead to scatter

In light of the form of Equation 2, where the half-length of the TWD contributes linearly to K_c , if the TWD increased in half-length due to stable tearing prior to instability, then the value of K_c increases proportionally, while the value of G_c on the y -axis of Fig. 3 increases as the square of that increase in half-length. Fig. 8 trends these dependencies as the basis to indicate the significant scatter that can develop due to the assumption that the pretest notch dimensions were a reasonable estimate of the circumstances at instability. The y -axis in this figure is the ratio of final to initial crack driving force while the x -axis is the amount of stable tearing normalized relative to the initial TWD half-crack length.

Fig. 8 indicates that where significant stable tearing is possible, the error introduced by using the initial TWD half-length in Fig. 3 can be several hundred percent. Critical in this context is that the resistance of the steel to stable tearing (quantified by CVN energy) and the initial notch depth couple nonlinearly to control the amount of tearing that occurs. Thus, small initial defects in tougher steels can undergo significant tearing, while longer initial defects in less tough

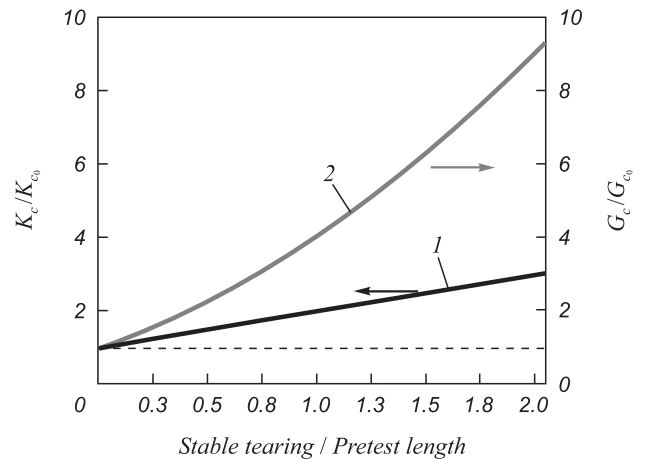


Fig. 8. Ratio of final to initial crack driving force as a function of normalized stable tearing:
1 – K_c ; 2 – G_c

steel undergo virtually no stable tearing. In regard to the TWD shown in Fig. 7, the final length (i.e., notch plus tearing) increased from 3.3 inches (84 mm) to about 5.6 inches (142 mm) prior to instability. Given this result, entering the x -axis in Fig. 8 at a value of $(5.6 - 3.3)/3.3 = 0.7$ indicates that for this test the value of G_c increased due to stable tearing by about 2.9 times.

It follows that the assumption that the pretest notch length was a reasonable estimate of the circumstances at instability by itself can lead to huge scatter in regard to Fig. 3. In view of this, the disparities evident in regard to the arrest toughness predictions in Fig. 6 versus that in Fig. 5 are not surprising. It is plausible in this context that the choice made to represent the results in Fig. 3 by a one-to one relationship provides an average outcome between cases that incurred significant stable tearing and those that did not. Another factor is that Test 18-8 was among the shortest pretest TWD lengths considered, and involved a steel capable of supporting significant stable tearing. This indicates that the 2.9 fold increase noted in the value of G_c tends to be a near worst-case indicator of the potential error due to this consideration. Finally, it is plausible that other assumptions or choices in parameter values act to offset the effects of this assumption. Regardless of which of these scenarios applies, it is clear that the value of G_c can vary greatly leading to scatter that can be expected in the use of the BTCM.

Toughness limitation for the BTCM and its consequences

As noted earlier, the calibration of the BTCM was limited to steels in Grade 448 (X65) and below that had $C_{v(1/1)}$ energy at 100 J or less. While it is usual to limit the use of any model that is empirically calibrated to within the bounds of the underlying database, because pipeline design is driven to more demanding applications there was an almost immediate need to use the BTCM beyond such bounds.

Trends as toughness increased – work in North America

The first practical test of the technology that underlies the BTCM came in the context of full-scale tests that were done in support of the Canadian Arctic Gas Study Limited (CAGSL). CAGSL involved a natural gas pipeline running from the North Slope of Alaska and the Mackenzie Delta, into the Northwest Territories, and on to Southern Canada and the United States. As the eventual design was not finalized in 1972 as the initial test parameters were being considered, that plan considered 48-inch (1219 mm) diameter line pipe produced in Grades 448 (X65) and 482 (X70) in wall thicknesses corresponding to an 80 % design factor. The plate rolled into test pipes involved both controlled-rolled and Q&T steels. The target pressure was 1680 psig (115.8 bar), which led to quite thick pipe. The target test temperatures were from -14 to -32 °F (-26 to -36 °C) to represent conditions considered relevant to the project. Consideration was given to integral ‘fracture arrestors’ in this set of tests. The second set of tests involved Grade 482 (X70) and was completed in 1975 under similar test conditions, except that slightly rich gas containing a modest amount of CO₂ was used. It follows that these tests were much more demanding than the circumstances considered for either the calibration database or the testing considered in regard to the BGC. As such, the toughness required to affect arrest for these tests was anticipated to run on average well above that of the full-scale test experience that was embedded in the calibration of the BTCM.

Although the initial testing was done in the early 1970s, and preceded the complete formulation of the BTCM (which was published in 1975), many of the key elements that underlie the BTCM had been published prior to or in 1972, in the context of the NG-18 Equations [e.g., 10, 11]. That technology was used to design the tests with the expectation that the range of toughness levels evaluated would arrest fracture at some level represented by the test pipes, yet only one of the pipes considered led to arrest. It follows that the technology that comprised the BTCM underestimated the arrest toughness of most of the test pipes. [e.g., 17] While many factors can conspire to produce this outcome, including the type of steels and low temperatures considered, the trend for the data was to underestimate the arrest toughness at toughness levels well beyond those previously experienced. In regard to Fig. 5 and 6, it is apparent that the toughness evident there on average is the order of 50 ft-lb or less, whereas the CAGSL test pipes had resistances often double that, which in one case ran in excess of 200 ft-lb (~270 J).

The next practical test for the BTCM came a few years after the first, with the testing done from 1979 through 1981. These full-scale tests were done in support of the Canadian segment of the Alaska Highway Gas Pipe Line (AHGPL) project, which was proposed to move natural gas south into Western Canada and on into the US. Thus, many of the test parameters targeted similar concerns as the CAGSL work,

except that they were AHGPL project-specific. This testing was done at the Northern Alberta Burst Test Facility (NABTF), with all testing done on Grade 482 (X70) line pipe in diameters as large as 56-inch (1219 mm), for wall thicknesses corresponding to an 80 % design factor. Target test pressures were as high as 1261 psig (86.9 bar), while the target test temperatures were from -6 up to 25 °F (-21 to -4 °C), being chosen to represent conditions considered relevant to the project. This work, which was finished in 1981, considered a range of slightly rich compositions, which in some cases contained a modest amount of CO₂. As for the CAGSL testing, these test conditions were much more demanding than the circumstances considered for either the calibration database or in the work for the BGC.

This testing was completed well after the BTCM was formulated and published. The reporting indicates that this technology was used to design the tests, which as noted above leads to the expectation that fracture would arrest well within the range of toughness levels used in the tests. The report [18] concludes that “the model (BTCM) provided predictions of arrest toughness that lay at the lower end of the observed range of arrest toughness” – so it follows that the BTCM underestimated the arrest toughness for many of the test pipes. As above, many factors can conspire to produce this outcome. And, as above, the arrest pipes had resistances often double that of the BTCM calibration database, which in one case exceeded 148 ft-lb (~200 J).

Trends as toughness increased – work in Europe

While not then apparent to those working at the NABTF to develop and analyze the data, a clear dependence of the BTCM predictions on toughness was emerging from the results of extensive full-scale testing done in Europe in the late 1970s and on into the early 1980s. As reported in 1983 [19], this work showed that the BTCM erred increasingly as the toughness increased beyond about 75 ft-lb (~100 J).

As time passed, it became clear that not only the BTCM and BSE results showed this trend, but that all SEs that had emerged to quantify fracture arrest for single-phase gases that were calibrated in reference to the CVN specimen shared the same trend: all became increasingly non-conservative as the toughness increased beyond about 75 ft-lb (~100 J) [20]. Fig. 9 illustrates this non-conservative ‘bent-over’ trend as the toughness required for arrest increases for predictions made using the AISI SE [8]. This tendency to underestimate required arrest toughness was evident for all grades evaluated. The results shown cover 120 arrests and 138 propagates in grades from X52 through X100, diameters from 24 to 56 inches (~406 to 1422 mm), wall thickness from 0.31 to 1.0 inch (7.95 to 25.4 mm), FSE CVN energies from 20 to 200 ft-lb (27 to 270 J), and pressures up to more than 2300 psi (16000 kPa).

The pipeline industry responds

The pipeline industry responded to the emergence of the trend to non-conservative predictions with two major

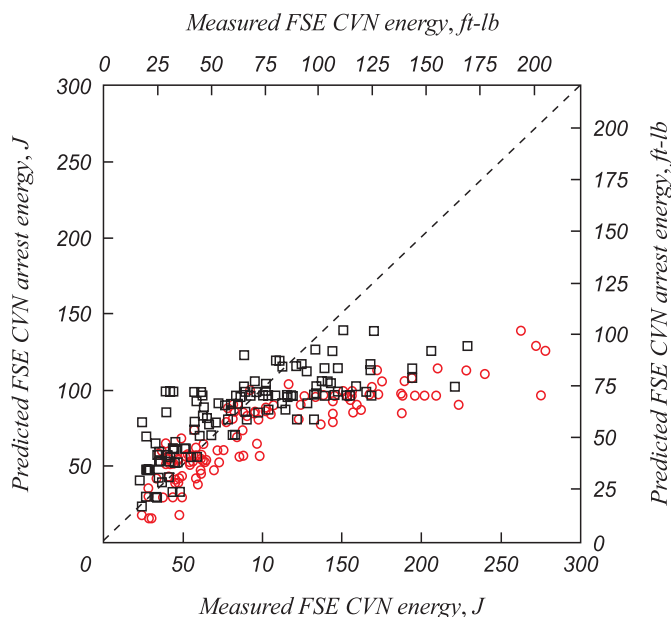


Fig. 9. Predicted arrest toughness requirements using the AISI SE:
 □ – propagate; ○ – arrest

thrusts. First, there was renewed interest in a better test to characterize fracture resistance. This action appears to represent the perceived inadequacy of the CVN Specimen as was evident in the consistent error made by all arrest models calibrated to CVN energy. Second, the industry began research to develop an alternative approach to characterize the crack driving force, as the basis to replace the BTCM with an ‘improved model’. In spite of related work [21] that indicated utility in the flow response of the steel and its relationship to the stretch local to the shear failure that is apparent in Fig. 2, the industry path forward eventually settled on NLFM. That choice apparently reflected the view that the significant developments in NLFM in the period since the BTCM emerged offered great promise, and the view that the phenomenology of this propagating shear failure apparent in Fig. 2 and 7 was fracture-controlled.

**Alternate fracture-based models:
 CTOA as a fracture metric**

Shortly after the consistent non-conservative predictive error for CVN-based models became evident, a major effort was initiated to develop alternative technology. Work began in the US to that end under the auspices of the PRCI in 1984 [22]. About the same time, a major effort with a comparable purpose had begun in Italy, with that work focused at Società NAzionale Metanodotti (SNAM) [23]. Collaboration between those efforts eventually ensued that sought to better characterize both the driving force for ‘running fracture’ and its resistance using a consistent fracture metric for both. The primary focus of that work was the evolution of crack-tip opening angle (CTOA) as a measure of the driving force for fracture [24] as well as its resistance [25].

Related work continues today, although the work that began at SNAM has now shifted to Centro Sviluppo Materiali (CSM).

Values of CTOA to arrest fracture based on those developments have from time to time been blind-predicted, which provides a basis to assess its progress toward a practically useful accurate predictor of arrest versus propagate as a function of CTOA. One such blind prediction well known to the author occurred in the context of the Alliance Pipeline, circa the mid-1990s. This blind numerical prediction, which came more than 10 years after that work began, indicated arrest at a CTOA on the order of 25° for this advanced-design pipeline [26]. This was in stark contrast to the largest published experimentally measured values of CTOA for then available steels that were the order of just 10°. While the very high predicted value of required CTOA in comparison to that for available steels was cause for pause, the full-scale testing went forward. In contrast to the blind predictions, those tests indicated arrest at value of CTOA that could be easily achieved for then available steels. Surprisingly to some, the CVN prediction based on the BTCM coupled with the LCF predicted the arrest toughness within a few percent – for all four arrests. These results led to reformulation of the CTOA model and redefinition of CTOA and its measurement practice. Thereafter, the required CTOA was still higher than the value evident in the testing inferred from CVN trending, but at about 12° [27] was much closer to the actual arrest conditions based on trending of the published CVN-CTOA results.

Related work by others involving CTOA has focused on a much different practice to measure this parameter, which after about five years of work appeared to hold promise [28]. However, after some additional work this activity drew to a close without apparent success. Others have sought to isolate crack propagation resistance in the context of CTOA (and other fracture-based metrics), coupling that effort with work related to testing practices to characterize fracture resistance. Schemes to isolate crack propagation resistance have focused on: 1) the notch configuration or its processing, 2) the back surface opposite the notch, and 3) the related test practice or specimen geometry. This work has likewise drawn to a close without success. Quite possibly the reason for this is because their focus was the energy dissipated only due to the creation of new fracture surface in propagation, whereas flow-controlled deformation in the context of Reference 21 appears to dominate the energy dissipated leading to the arrest of propagating shear in a pipeline.

It follows that schemes to characterize shear propagation in a pipeline and the steel’s resistance to that process have been attempted using fracture-based concepts since the late 1960s. CTOA as a metric of fracture has been in development now for a period of almost three decades – but as yet a simple practical model CTOA-based model such as the BTCM has not emerged.

Other recent work: fracture control for the alliance pipeline

Background

The proposed Alliance Pipeline design involved a novel dense-phase compression and transport concept [29] that would move the richest (dense-phase) gas yet considered through a large (36 inch / 914 mm) diameter pipeline operating at 1740 psig (~120 bar). While Grade 551 (X80) was considered early in the design process, eventually Grade 482 (X70) was proposed working at 80 % design factor, which was allowable and usual for cross-country service in Canada. Given the issues evident in predicting arrest toughness for the full-scale testing done prior to the mid-1990s, developing the fracture control plan (FCP) for any pipeline posed a problem if its design concept and operational parameters lay outside the scope of the available full-scale testing. On this basis, the design pressure and other aspects advanced-design Alliance Pipeline placed it well outside the scope of that full-scale database. As such, a means to address the just-noted issues was required if this design was to go forward, which because that means was unproven for those design conditions would need to be validated by successful full-scale testing.

Managing the effects of increasing toughness

Not surprisingly, the predicted arrest toughness for the Alliance Pipeline based on the BTCM was above the 75 ft-lb (~100 J) limit beyond which Fig. 9 shows this model is increasingly non-conservative. Because the other CVN-based methods also showed this same tendency as had been evident for the BTCM, and the use of CTOA had not yet been proven by successful blind predictions of fracture arrest, developing the FCP for this pipeline posed a major challenge. Alternative schemes were sought by the Alliance Consortia. Eventually, consideration given to an emerging concept developed under IR&D funding at Battelle in the early 1990s [13], which provided a physically sound basis to offset the cause for the ‘bent-over’ trend seen in Fig. 9.

Differences in the inherent fracture resistance of a CVN specimen were evaluated as the FSE CVN energy increased from a low of 18 ft-lb (24 J) to a high of 260 ft-lb (352 J) in steels from Gr B up to X80, which were produced from the 1960s into the early 1990s. Using results from instrumented CVN testing, dissipation was separated into fracture initiation, plastic deformation, and fracture resistance. Fig. 10 trends the shift in energy dissipation in the CVN specimen for each of the initiation, plastic deformation, and propagation components.

The y-axis in Fig. 10 is the fraction of the energy dissipated in the above-noted components as a function of total energy dissipated in the test, which is shown on the x-axis. These trends were normalized relative to the trend developed in testing up through 75 ft-lb (~100 J), with a best-fit function developed from that process that predicts the shortfall in the BTCM predicted energy due to differences

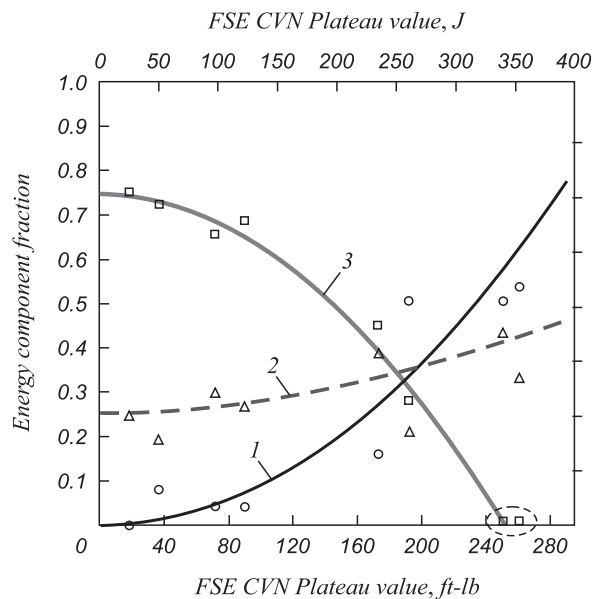


Fig. 10. Shift in CVN dissipation for the initiation, plastic deformation, and propagation components as total energy increases: 1 – Trend D; 2 – Trend I; 3 – Trend P; □ – propagate; ○ – deformation; Δ – initiation

in the response of the CVN specimen as toughness increases. Of significance in these trends is the observation that for these steels the propagation component approaches zero at about 250 ft-lb (~339 J). In turn, this means that the CVN test loses its utility in the context of its historic purpose in the BTCM formulation at energy levels of that order, and above.

Recognizing that the CVN test loses its utility in the context of its historic purpose in the BTCM at energy levels the order of 250 ft-lb (~339 J) and above, it follows that one must question specifying steels relative to CVN testing at high energy levels. It also follows that trends between predicted and actual arrest energy levels that develop and can be quantified functionally at lower energy levels are likely to breakdown completely as they approach much less exceed a FSE CVN energy level of 250 ft-lb (~339 J). The results showed that the ratio of the initiation (plus deformation) energy to the propagation energy in a CVN specimen was inherently different for high toughness steels as compared to that for low toughness steels, and that the energy dissipated in initiation increased with toughness, as did that for plastic deformation. Based on these observations and the energy dissipation principle, a correction was developed for the BTCM as the basis to predict the CVN energy to arrest shear propagation for the Alliance Pipeline. Over the course of the Alliance Pipeline Certification Hearing [30] this correction became known as the ‘Leis correction factor’.

Outcomes using the leis correction factor

As evident in Fig. 11, when applied to predictions for the same database considered in Fig. 9, the LCF effectively offsets the non-conservative nature of the BTCM for the higher toughness steels in that database. These data run to

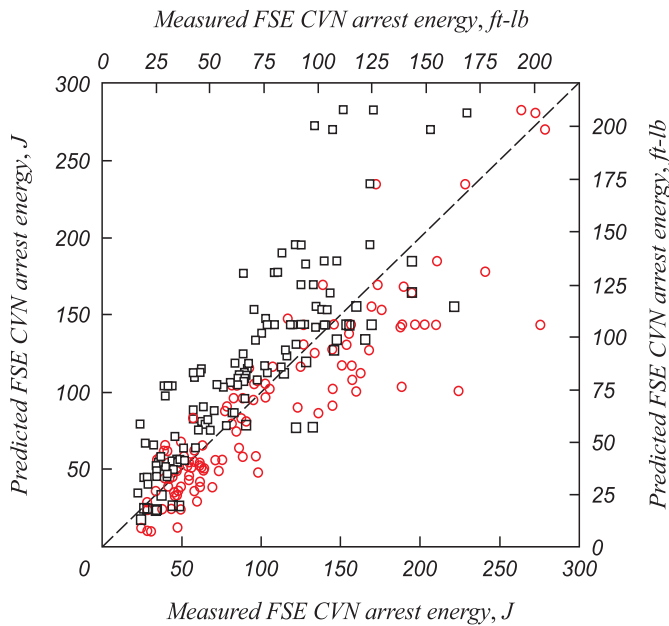


Fig. 11. Leis correction factor applied with the BTCM to the test results in Fig. 9:
 □ – propagate; ○ – arrest

quite high toughness levels (≤ 270 J), all of which reflect single-phase decompression. Given this outcome, blind predictions also were made for the planned full-scale testing to validate this correction for use with the Alliance Pipeline design and FCP. As noted earlier, and discussed in more detail later, it was found that the corrected BTCM predictions matched the observed arrest toughness within a few percent of each other for each of four arrests, while CTOA as noted above was not validated by that testing.

It follows that the LCF provided a rational approach to extend the utility of the BTCM to much higher toughness levels. However, as has been made clear in related work, this correction is empirically calibrated for up to Grade 551 (X80), and toughness levels the order of ~ 225 ft-lb (~ 305 J), but validated only for Grade 482 (X70) and below. Note too that the LCF also reflects a range of steels whose flow and fracture response both contributed to its successful use.

Recognizing the lesson discussed earlier in regard to using the BTCM beyond its empirical basis, the LCF does not provide a general path forward – nor do any of the other correction factors that followed in the wake of the LCF. Rather, technology must be developed that addresses the inadequacies of what is currently available as 1) the toughness continues to increase, 2) the flow response shifts to higher values of Y/T , and 3) the specimens used to quantify resistance to propagating shear become less effective.

Challenge posed by high-toughness high-strength grades

The economics of pipeline construction and operation motivate the development of higher-strength grades, which fall well above the empirical basis for the current fracture

arrest technology and require full-scale testing to assess the viability of the steels considered for a given pipeline design. The development of microalloyed steel and the role played by Niobium remains critical in keeping pipelines cost competitive, while at the same time leading to steel that is weldable, as well as strong and tough, and so capable of satisfying the requirements of strain-based design. Gray [31] tracks the evolution of steel and makes clear the benefits of Niobium in line-pipe applications. While the benefits are understood, without a means to specify the toughness required to arrest fracture, and to quantify what level is required for a given pipeline, it will be difficult to capitalize on those benefits without a complete understanding of propagating shear, and a means to quantify that arrest is certain in the event that such a failure initiates.

Realizing that advanced-design pipelines will require high-toughness if they are to avoid the use of fracture arrestors, and that toughness continues to be quantified by CVN energy, the steel industry has learned to produce steels that seem designed to ‘stop the hammer’ in CVN testing. Such steels are marketed today with toughness levels approaching 500 ft-lb (678 J). In view of the trends in Fig. 10, one must question the value of ‘arrest’ resistance approaching or above 250 ft-lb (339 J). Further reason to question the merits of toughness at such levels derives from Fig. 12. Fig. 12 summarizes the results of full-scale testing done by CSM [32] primarily in regard to Grade 551 (X80) and Grade 689 (X100), with limited data also for Grade 827 (X120). The format of this figure is comparable to Fig. 9 and 11. Fig. 12, *a* is based on predictions by the BTCM whereas Fig. 12, *b* presents BTCM predictions with the LCF.

Fig. 12, *a* looks much like the BTCM predictions shown earlier in Fig. 9, which as noted then included data for grades up to EX100, all of which were produced with practices used prior to ~ 1990 . It shows the same bent-over trend, which develops beyond about 100 J (~ 75 ft-lb). In view of the utility of the LCF evident in Fig. 11, it is conceivable that the LCF can affect improved predictions as well in regard to these data for higher-strength grades using steels made with much different practices when compared to that of the 1970s and before. However, as has been noted in prior discussion, the dissipation response embedded in the LCF as well as the flow response embedded in the calibration of the BTCM differ from trends for that evident with recent production. The effects of these differences are apparent in the data presented in Fig. 13, which shows Y/T as a function of SMYS in Fig. 12, *a* and AYS in Fig. 12, *b*. Results for AYS are included along with that for SMYS as the ratio of AYS/SMYS also has been decreasing.

The BTCM was formulated by relating the ‘fracture’ speed to that of the plastic wave speed, where the latter is proportional to the slope of stress-plastic strain curve. If the trend through the results in Fig. 13, *a* is considered typical and combined with related data for the strain to failure, then that slope for the X70 grade steels is \sim six times that for the

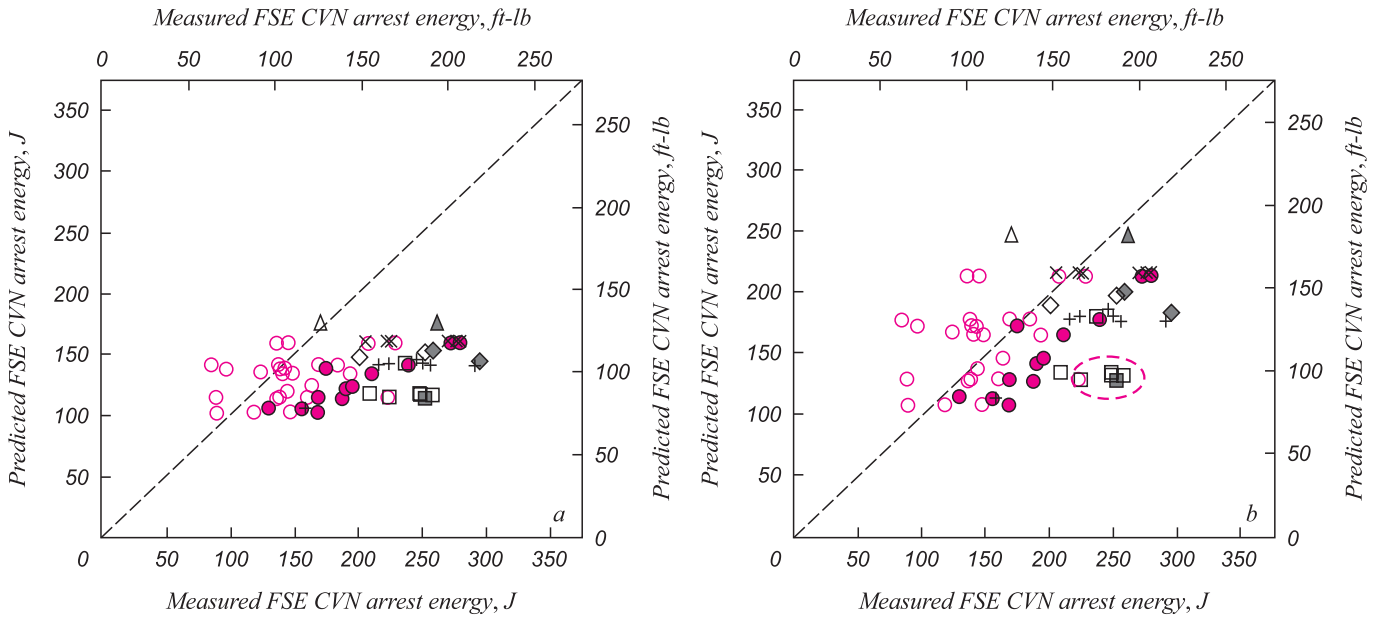


Fig. 12. CSM database for X80 and X100 tests (data from Reference 32):

a – BTCM predictions for high-grade steels; *b* – BTCM-LCF predictions for high-grade steels; ● – X80 A – CSM Database; ○ – X80 P – CSM Database; ▲ – X100 A – 1st ECSC; △ – X100 P – 1st ECSC; ◆ – X100 A – 2nd ECSC; ◇ – X100 P – 2nd ECSC; ■ – X100 A – 1st Demopipe; + – X100 P – 1st Demopipe; □ – X100 P – 2nd Demopipe; × – X120 P – ExMob

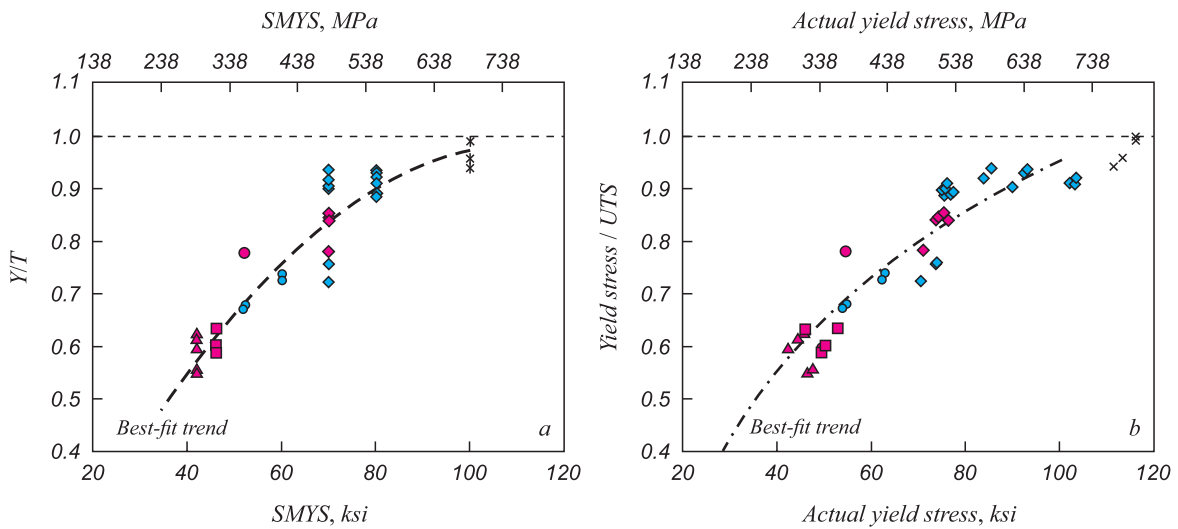


Fig. 13. Trends in the flow properties represented by Y/T with Grade (archival data):

a – as a function of SMYS; *b* – as a function of AYS; ▲ – 40s vintage X42; ■ – 40s vintage X46; ● – 40s vintage X52; ● – 50s–60s vintage X52 – X56; ◆ – Early 80s vintage X70; ◆ – archives modern X70 & up; * – late 1990s X100; × – late 1990s X100 (EC2–3)

X100 steels. This difference indicates that 1) the BTCM is likely to underestimate the required arrest resistance and 2) it is unlikely the BTCM coupled with the LCF will be as effective in offsetting the ‘bent-over’ trend as evident for Fig. 11 in predictions for data from the era that the BTCM was formulated. Inspection of Fig. 12, *b* confirms this expectation: while some improvement is evident through the use of the LCF, many results remain in error.

Close study of Fig. 12, *b* for cases involving high fracture resistance indicates that the data for pipes that arrest propagating shear becomes comingled with those that permit continued propagation. In addition to being comingled, such results span a significant range of CVN resistance –

with failure effectively independent of CVN. Examples of comingled data can be seen in the two sets of points circled at about 250 J, while the results for the 1st ‘Demopipe’ test that show propagation at more than 350 J (~260 ft-lb) illustrate independence of CVN energy. This means that for these types of steels the CVN energy no longer discriminates effectively between pipes that arrest versus pipes that propagate shear failure – particularly at high resistance. In view of this trend, one could assert that a toughness level exists beyond which the failure process transitions from fracture control to collapse control: beyond that level running ‘fracture’ is a propagating tensile instability rather than an extending crack.

Until we fully understand the factors that drive propagating shear, we cannot logically develop the means to quantify the factors that control its arrest, and establish reliable measures of the steel's resistance to such failure. Full-scale testing provides a stopgap until that understanding evolves, but such testing is expensive and of limited general utility, as the result from a given test is specific to the test parameters considered. It follows that a technology-based relationship is needed if tough strong steels are to be broadly marketed as the means to economically expand access to environmentally friendly sources of energy like natural gas.

While the LCF extended the utility of the BTCM for a few years covering some higher-strength grades produced in the new Millennium, in many ways the need to characterize relationships between pipeline design parameters and the arrest of propagating shear remains today much as it has since the late 1960s. Formally dealing with the flow and fracture behavior, the decompression behavior, and the soil-structure or water-structure interaction that contribute to the failure response requires quantifying complex interacting nonlinearities. This has proven problematic without recourse to semi-empirical approaches. Uncoupling these three nonlinearities as a basis to numerically characterize their effects independently, and to validate those outcomes prior to reintegrating their coupled effects, is a daunting and expensive process.

Uncoupling the nonlinearities in a fundamental way will require expensive experiments that physically isolate each of the nonlinear processes, which will likely require instrumented, well designed above-ground full-scale testing. While such work could prove instructive, the fact remains that attempts to use fracture-based methods to characterize shear propagation in a pipeline and the steel's resistance to that process have been pursued since the late 1960s. More advanced fracture-based concepts, such as CTOA, likewise have been in development as metrics for fracture for a period that now is almost three decades. In spite of the tens of millions invested to date in theory and related experiments, as yet a simple practical model, such as the BTCM, has not emerged through work founded on fracture-based technologies.

Fracture has been an appealing basis to characterize ductile propagating shear, and seemed logical as this failure process emerged in the wake of brittle propagating fracture. However, after 40 years in pursuit of a fracture-based approach without success in the form of a simple model like the BTCM it seems reasonable to reassess the phenomenology. The key question is – where to start?

The end of the article in the next issue.

REFERENCES

1. Broek D. *Elementary Engineering Fracture Mechanics*. Noordhoff, 1974; see also Hertzberg R.W. *Deformation and Fracture Mechanics of Engineering Materials*. John Wiley and Sons, 1976.

2. Irwin G.R. Analysis of Stresses and Strains Near the End of a Crack Traversing a Plate. *J of App Mech*, ASME, vol. 24, 1957, pp. 361–364.
3. Maxey W.A. Fracture Initiation, Propagation, and Arrest. Paper J. 5th Symposium on Line Pipe Research, *PRCI Catalog*. no. L30174, November 1974.
4. Starling K.E. *Fluid Thermodynamic Properties for Light Petroleum Systems*. Texas: Gulf Publishing Co., 1973.
5. Hopke S.W., Lin C.J. Applications of the BWRs Equation to Natural Gas Systems, paper presented at the 75th National AIChE Meeting, Denver, March 1974.
6. Eiber B., Leis B., Carlson L., Horner A., Gilroy-Scott A. Full-Scale Tests Confirm Pipe Toughness for North American Pipeline. *O&GJ*, vol. 97, no. 45, November 8, 1999, pp. 48–54.
7. Maxey W.A., Kiefner J.F., Eiber R.J. Ductile Fracture Arrest in Gas Pipelines. AGA NG-18 Report 100, *PRCI Catalog*. no. L32176, 1975.
8. anon. *Running Shear Fractures in Line Pipe*, AISI Subcommittee of Large Diameter Line Pipe Producers, AISI Technical Report, 1974.
9. Priest A.H., Holmes B. *The Characterization of Crack Arrest Toughness in Gas Transmission Pipelines in Terms of Shear Fracture Propagation Energy (BSC Criterion)* Final Report on ECSC Agreement 7210-KE/808, December 1985.
10. Kiefner J.F., Maxey W.A., Eiber R.J., Duffy A.R. *Failure Stress Levels of Flaws in Pressurized Cylinders*. ASTM Special Technical Publication (STP) 536, American Society for Testing and Materials, 1973, pp. 461–481; see also Maxey W.A., Kiefner J.F., Eiber R.J., Duffy A.R. *Ductile Fracture Initiation, Propagation, and Arrest in Cylindrical Vessels*. ASTM STP 514, 1972.
11. Hahn G.T., Sarrate M. and Rosenfield A.R. Criteria for Crack Extension in Cylindrical Pressure Vessels. *I J Frac Mech*, vol. 5, 1969, pp. 187–210.
12. Kawaguchi S., Hagiwara N., Ohata M., Toyoda T. Modified Equation to Predict Leak/Rupture Criteria for Axially Through-wall Notched X80 and X100 Line pipes Having Higher Charpy Energy. *Proceedings 5th International Pipeline Conference*, ASME, Calgary, 2004, IPC04-0322.
13. Leis B.N. *Relationship Between Apparent Charpy Vee-Notch Toughness and the Corresponding Dynamic Crack-Propagation Resistance*. Battelle Report to R.J. Eiber, Consultant, Inc., 1997; available as Appendix C; Exhibit B-82, Proceeding GH 3-97, National Energy Board of Canada, 1997–1998.
14. Leis B.N., Zhu K-K. *Leak vs. Rupture Boundary for Pipes with a Focus on Low Toughness and/or Ductility*. PRCI Final Report on Project EC2-3, April 16, 2012.
15. Maxey W.A. Dynamic Crack Propagation in Line Pipe, Plenary Lecture, *International Conference on Analytical and Experimental Fracture Mechanics*, Rome, June 1980.
16. Poynton W.A. A Theoretical Analysis of Shear Fracture Propagation in Backfilled Gas Pipelines, *Symposium on Crack Propagation in Pipelines*, The Institute of Gas Engineers, Newcastle Upon Tyne, England, March 1974.
17. Eiber R.J., Maxey W.A. Full-Scale Experimental Investigation of Ductile Fracture Behavior in Simulated Arctic Pipeline. *Proceedings of the Grey Rocks Symposium, Materials Engineering in the Arctic*, ASM, 1977, pp. 306–310.
18. Foothills Pipe Lines (Yukon) Ltd. Final Report on the Test Program at the Northern Alberta Burst Test Facility, Report 18031, Calgary, Canada, 1981.
19. Vogt G.H., etc. EPRG Report on Toughness for Crack Arrest in Gas Pipelines, *3R International*, vol. 22, 1983, pp. 98–105.
20. Leis B.N., Eiber R.J., Carlson L., Gilroy-Scott A. Relationship Between Apparent Charpy Vee-Notch Toughness and the Corresponding Dynamic Crack-Propagation Resistance, *1998 Int. Pipeline Conference*, Volume II, ASME Calgary, 1998, pp. 723–731.
21. Gray J.M. Ductile Fracture of Gas Pipelines: Correlation between Fracture Velocity and Plastic Zone, *NG-18 Report from MicroAlloying International*, MA/83/1, July 1983.
22. Kanninen M.F., O'Donoghue P.E., Cardinal J.W., Leung C.P., Morrow T.B., Green S.T., Popelar C.F. *Dynamic Fracture Mechanics*

- Analysis and Experimentation for the Arrest of Ductile Fracture Propagation in Gas Transmission Pipelines, in *Proc. Pipeline Technology Conf.*, (R. Denys, Editor), Oostende, Belgium, 1990, Part B, pp. 16.1–13.
23. Venzi S., Martinelli A., Re G., Celant M. Measurement of Fracture Initiation and Propagation Parameters from Fracture Kinematics. *Proc. Anal and Exp Fracture Mechanics*, Rome, 1980, pp. 737–756.
 24. Martinelli A., Venzi S. Tearing Modulus, J-Integral, CTOA, and Crack Profile Shape obtained from the Load Displacement Curve Only. *Engr. Fract. Mech.*, vol. 53, no. 2, 1996, pp. 263–277.
 25. Demofonti G., Buzzichelli G., Venzi S. and Kanninen M.F. “Step by Step Procedure for the Two Specimen CTOA Test”, *Proc. 2nd Conf. On Pipeline Technology*, vol. II, pp. 503–512, Elsevier, 1995.
 26. *SWRI-CSM, CTOA for Fracture Arrest in Alliance Pipeline*, via private communication between C.W. Peterson and E.L. Von Rosenberg, Consultant to Alliance Pipeline, March 1997.
 27. Mannucci G. *Written report (CSM Ref. NM90187)* via private communication with R.J. Eiber, Consultant to Alliance Pipeline, December, 1999.
 28. Hashimi S.H., Howard I.C., Yates J.R., Andrews R.M., Edwards A.M. A Specimen for Studying the Resistance to Ductile Crack Propagation in Pipes, *5th Int. Pipeline Conference*, IPC04-0610, Calgary, 2004.
 29. Janzen T.S., Horner W.N. The Alliance Pipeline – a Design Shift in Long Distance Gas Transmission. *1998 Int. Pipeline Conf.*, ASME, pp. 83–88, 1998.
 30. Leis B.N. *Archives Canadian Nat. Energy Board*, GH-3-97, vol. 45, 1997.
 31. Gray J.M. *An Independent View of Linepipe and Linepipe Steel for High Strength Pipelines: How to Get Pipe that's Right for the Job at the Right Price*, presented at the API X-80 Pipeline Cost Workshop, Hobart, Australia, October 2002.
 32. Demofonti G., Mannucci G., Di Biagio M., Hillenbrand H-G., Harris D. Fracture Propagation Resistance of X100 TMCP steel Pipes for High-Pressure Gas Transmission Pipelines using Full-Scale Bursts, *3rd Pipeline Technology Conf.*, vol. 1, Scientific Surveys, 2004, pp. 467–482.

© 2015 Leis B.N.
Received October 29, 2014

ПРИОСТАНОВЛЕНИЕ РАСПРОСТРАНЕНИЯ ДЕФОРМАЦИИ В МАГИСТРАЛЬНОМ ТРУБОПРОВОДЕ

Брайан Н. Лейс, д.т.н., консультант
(bleis@columbus.rr.com)

(517, Пое стр., Уоррингтон, штат Огайо, 43085-3036, США)

Аннотация. Для проявления распространяющегося пластического разрушения требуется, чтобы трубопроводы были спроектированы с учетом недопущения распространения трещин. Подходы, описывающие поведение трубопровода, его устойчивость и гарантированную остановку в случае сбоев в работе, основаны на полуэмпирических моделях, получивших свое развитие в середине 1970-х годов. Эти модели, которые калибровались на сегментах трубопровода в производственном масштабе (в натуральную величину), используются и сейчас, и включают три нелинейные

характеристики: пластическую деформацию и винтовую неустойчивость; влияние структуры (состава) почв и увеличение волновой отдачи, а также декомпрессию в нагнетающей среде. Рассматривается более чем 40-летняя история расчета распространения деформации в трубопроводе, основанного на трещинах (механическом разрушении). Графические свидетельства полномасштабных сбоев в процессе работы обусловили появление гипотезы о сбоях, возникших в связи и пластическим разрушением.

Ключевые слова: распространение деформации, трещина, приостанавливать, вязкая сталь, степень пластичности, сталь, разделение/расщепления, разработка модели.

Список литературы см. выше.

Получена 29 октября 2014 г.